Imprints of molecular orbitals using photoelectron angular distribution by strong laser pulses of circular polarization*

Ren Xiang-He(任向河)[a)†], Wu Yan(吴 艳)[b)], Zhang Jing-Tao(张敬涛)[c)‡], Ma Hui(马 慧)[a)], and Xu Yu-Long(许玉龙)[a)]

[a)] School of Sciences, Shandong Polytechnic University, Jinan 250353, China

[b)] Department of Physics, Zhejiang University of Science & Technology, Hangzhou 310018, China

[c)] State Key Laboratory of High Field Laser Physics, Shanghai Institute of Optics and Fine Mechanics, Chinese Academy of Sciences, Shanghai 201800, China

(Received 12 December 2012; revised manuscript received 21 January 2013)

We theoretically investigate the strong-field ionization of H_2^+ molecules in four different electronic states by calculating photoelectron angular distributions in circularly polarized fields. We find that the structure of photoelectron angular distribution depends on the molecular orbital as well as the energy of the photoelectron. The location of main lobes changes with the symmetric property of the molecular orbital. Generally, for molecules with bonding electronic states, the photoelectron's angular distribution shows a rotation of $\pi/2$ with respect to the molecular axis, while for molecules with antibonding electronic states, no rotation occurs. We use an interference scenario to interpret these phenomena. We also find that, due to the interference effect, a new pair of jets appears in the waist of the main lobes, and the main lobes or jets of the photoelectron's angular distribution are split into two parts if the photoelectron energy is sufficiently high.

Keywords: photoelectron angular distributions, circular polarization laser field, photoionization, molecule

PACS: 33.80.Rv, 32.80.Rm, 34.50.Gb, 42.50.Hz **DOI:** 10.1088/1674-1056/22/7/073304

1. Introduction

Recently, photoionization of atoms and molecules in intense laser fields has attracted much attention.[1–7] Because the outgoing photoelectrons from photoionization carry the information of atomic and molecular orbitals, studies on photoionization enrich our knowledge of the atomic and molecular structures as well as the physical process itself. Moreover, because molecules have more degrees of freedom that affect the strong-field ionization than atoms, photoionization of molecules in a strong field becomes a more attractive means of disclosing the molecular structures. In the strong-field ionization processes of molecules, the final kinetic energy and the emission direction of photoelectrons can be experimentally observed. Hence, the photoelectron spectroscopy becomes available. The photoelectron angular distribution (PAD) is one kind of these photoelectron spectroscopies. In our previous work,[8–10] regarding the PADs of molecules, we found that, in contrast to using laser fields of linear polarization, the usage of circular polarization has two unique advantages. (i) The PADs of molecules in laser fields with either linear or circular polarization are decided by the molecular electronic state, the number of absorbed photons, and the laser parameters including laser intensity and laser frequency. The PADs in the presence of linearly polarized lasers vary sensitively with the laser parameters and the number of absorbed photons,[11] so it is difficult to control the PADs in a linearly polarized laser field. The PADs in the case of circular polarization, however, are very stable against the laser parameters and the number of absorbed photons. (ii) The electric vector of circularly polarized laser fields rotates around the wave vector with a constant amplitude, which means that the electric field is uniformly distributed in the radial direction. Thus, the subsequent motion of photoelectrons after ionization is changed less by the laser field, and then the PADs directly reflect the molecular orbital. Apart from these two special advantages, it is generally accepted that the rescattering effect by circular polarization is weak, which entails a cleaner signal with respect to the molecular orbital. Due to these advantages, the PADs with circular polarization directly provide clear information of molecular orbitals, so the PAD becomes a simple tool to investigate the molecular orbital.[12–17]

Among all molecules, the H_2^+ molecule is of special importance. This molecule contains only one electron, so the multi-electron effects during photoionization are avoided. The initial state of the H_2^+ molecule can be obtained analytically by the linear combination of atomic orbitals (LCAO),[18] so the complex computation needed to obtain molecular wave functions is also avoided. Hence, the photoionization of H_2^+ molecule attracts many theoretical efforts.[19–23] Experimentally, the H_2^+ molecule can be obtained from the ionization of

*Project supported by the National Natural Science Foundation of China (Grant Nos. 11104167, 11174304, and 61078080), the Excellent Middle-Aged and Youth Scientist Award of Shandong Province, China (Grant No. BS2011SF021), and the Scientific Research Foundation for the Returned Overseas Chinese Scholars.

†Corresponding author. E-mail: xhren101@spu.edu.cn

‡Corresponding author. E-mail: jtzhang@siom.ac.cn

© 2013 Chinese Physical Society and IOP Publishing Ltd

H_2 molecule, and several electronic states are available. One must recognize that the dissociation of H_2^+ will happen after the first electron of H_2 is ionized. Moreover, it is noteworthy that the current treatment can be extended to more complicated molecules, such as homonuclear molecules (N_2, O_2), the heteronuclear molecules (NO, CO), and even polyatomic molecules.

In this paper, we calculate the three-dimensional PADs (3D-PADs) of the molecule H_2^+ in four electronic states. We focus on the issue of how the PADs vary with the molecular orbital and the photoelectron energy. We will show that the structure of PADs depends on the molecular orbital as well as the energy of the photoelectron.

2. Model and method

To theoretically study the photoionization process of atoms and molecules in intense laser fields, the strong-field approximation (SFA) is commonly used.[24–27] In this treatment, the Coulomb attraction between the parent ion and the ionized electrons is ignored, and the state of the electrons in intense laser fields is described by a Volkov state.[28] Within the SFA, the ionization rate in strong laser fields is given by[24,27,29] ($c = \hbar = 1$ are used throughout this paper)

$$\frac{\mathrm{d}W}{\mathrm{d}\Omega_{\boldsymbol{P}_\mathrm{f}}} = \frac{(2m_\mathrm{e}^3\Omega^5)^{1/2}}{(2\pi)^2}\sum_{n=n_0}\left(n-u_\mathrm{p}\right)^2\left(n-u_\mathrm{p}-\varepsilon_\mathrm{b}\right)^{1/2} \times |\mathscr{J}_n(Z_\mathrm{f})|^2\,|\Psi(\boldsymbol{P}_\mathrm{f},\boldsymbol{R})|^2, \quad (1)$$

where $\mathrm{d}\Omega_{\boldsymbol{P}_\mathrm{f}} = \sin\theta_\mathrm{f}\mathrm{d}\theta_\mathrm{f}\mathrm{d}\varphi_\mathrm{f}$ is the differential solid angle of the momentum of photoelectron ($\boldsymbol{P}_\mathrm{f}$, $|\boldsymbol{P}_\mathrm{f}| = \sqrt{2m_\mathrm{e}\Omega(n-u_\mathrm{p}-\varepsilon_\mathrm{b})}$), θ_f and φ_f are the polar and azimuthal angles, m_e is the electron mass, $\varepsilon_\mathrm{b} = E_\mathrm{b}/\Omega$ is the molecular binding energy (E_b) in the unit of laser-photon energy (Ω), n is the number of absorbed photons, $n_0 = \left(u_\mathrm{p}+\varepsilon_\mathrm{b}\right)_\mathrm{int}+1$ is the minimum number of photons absorbed for ionization, and $u_\mathrm{p} = U_\mathrm{p}/\Omega$ is the ponderomotive parameter of the laser fields, which is defined as

$$u_\mathrm{p} = \frac{e^2 I}{2m_\mathrm{e}\Omega^3},$$

with I being the laser beam intensity. The argument of Bessel function in Eq. (1) is defined as

$$Z_\mathrm{f} = \frac{e\sqrt{2I}}{m_\mathrm{e}\Omega^2}\boldsymbol{\varepsilon}\cdot\boldsymbol{P}_\mathrm{f}, \quad (2)$$

where $\boldsymbol{\varepsilon}$ is the polarization vector of the laser field,

$$\boldsymbol{\varepsilon} = \boldsymbol{\varepsilon}_x\cos\frac{\xi}{2} + \mathrm{i}\boldsymbol{\varepsilon}_y\sin\frac{\xi}{2}, \quad (3)$$

and $\xi = \pi/2$ for the circular polarization. Combining Eq. (2) and Eq. (3), the argument Z_f in Eq. (1) for circular polarization can be written as

$$Z_\mathrm{f} = \frac{e\sqrt{I}P_\mathrm{f}}{m_\mathrm{e}\Omega^2}\sin\theta_\mathrm{f}\,\mathrm{e}^{\mathrm{i}\varphi_\mathrm{f}}. \quad (4)$$

In Eq. (1), $\Psi(\boldsymbol{P}_\mathrm{f},\boldsymbol{R})$ is the Fourier transformation of the initial wave function of the molecule ($\Phi_\mathrm{i}(\boldsymbol{r},\boldsymbol{R})$), where $\boldsymbol{R}$ is the molecular vector, $|\boldsymbol{R}|$ is the internuclear distance of the molecule, and $\boldsymbol{r}$ denotes the position vector of the electron with respect to the center of mass of the molecule (see Fig. 1(a)). We take $1s\sigma_\mathrm{g}$, $1s\sigma_\mathrm{u}$, $2p\pi_\mathrm{u}$, and $2p\pi_\mathrm{g}$ as the initial states. According to the LCAO theory,[18] the two-centered single-electron molecular wave function can be expressed as an appropriate superposition of scaled 1s and 2p atomic orbitals of hydrogen, and has the following form:[30,31]

$$\Phi_\mathrm{i}(\boldsymbol{r},\boldsymbol{R}) = \frac{\Phi_{(h)}(\boldsymbol{r}-\boldsymbol{R}/2)\pm\Phi_{(h)}(\boldsymbol{r}+\boldsymbol{R}/2)}{\sqrt{2\left[1\pm S_{(h)}(R)\right]}},$$

where the plus sign corresponds to $1s\sigma_\mathrm{g}$ and $2p\pi_\mathrm{u}$ states, and the minus sign corresponds to $1s\sigma_\mathrm{u}$ and $2p\pi_\mathrm{g}$. The atomic orbital overlap integral, $S_h(R)$, is defined as

$$S_h(R) = \int \mathrm{d}\boldsymbol{r}\,\Phi_{(h)}(\boldsymbol{r}-\boldsymbol{R}/2)\Phi^*_{(h)}(\boldsymbol{r}+\boldsymbol{R}/2).$$

Here, h represents 1s or 2p.

After the Fourier transformation, the molecular wave functions in momentum space are derived to be

$$\Psi^{(1s\sigma_\mathrm{g})}_{(1s\sigma_\mathrm{u})}(\boldsymbol{P}_\mathrm{f},\boldsymbol{R}) = \frac{\Phi_{(1s)}(\boldsymbol{P}_\mathrm{f})}{\sqrt{2\left[1\pm S_{(1s)}(R)\right]}}\begin{cases}\cos(\boldsymbol{P}_\mathrm{f}\cdot\mathbf{R}/2)\\ \sin(\boldsymbol{P}_\mathrm{f}\cdot\mathbf{R}/2)\end{cases}, \quad (5)$$

$$\Psi^{(2p\pi_\mathrm{u})}_{(2p\pi_\mathrm{g})}(\boldsymbol{P}_\mathrm{f},\mathbf{R}) = \frac{\Phi_{(2p)}(\boldsymbol{P}_\mathrm{f})\sin(\varphi_\mathrm{p})}{\sqrt{2\left[1\pm S_{(2p)}(R)\right]}}\begin{cases}\cos(\boldsymbol{P}_\mathrm{f}\cdot\mathbf{R}/2)\\ \sin(\boldsymbol{P}_\mathrm{f}\cdot\mathbf{R}/2)\end{cases}, \quad (6)$$

where $\Phi_{(1s)}(\boldsymbol{P}_\mathrm{f})$ and $\Phi_{(2p)}(\boldsymbol{P}_\mathrm{f})$ are the Fourier transformation of the atomic wave functions $\Phi_{(1s)}$ and $\Phi_{(2p)}$, respectively, and φ_p is the angle of photoelectron momentum with respect to the molecular axis. The trigonometric functions, $\sin(\boldsymbol{P}_\mathrm{f}\cdot\mathbf{R}/2)$ and $\cos(\boldsymbol{P}_\mathrm{f}\cdot\mathbf{R}/2)$, describe the interference, which stems from the double-core feature of the molecule.[24,32] We use θ_R and φ_R to denote the polar and azimuthal angles of the molecular axis, as shown in Fig. 1(a). The z axis is along the propagation direction of the laser field. Such treatment can be extended to more complicated molecules, such as homonuclear molecules N_2 and O_2, heteronuclear molecules NO and CO, and even polyatomic molecules.

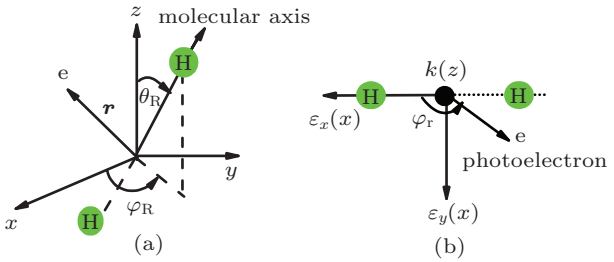


Fig. 1. (color online) (a) Coordinate system for H_2^+ molecule in the ground state without laser fields. (b) Coordinate system for H_2^+ molecule upon photoelectron ejection. The molecule is supposed to be in the polarization plane.

3. Numerical results and discussion

In our calculations, the circularly polarized laser field's wavelength is 0.8 μm, with its intensity varying from 10^{14} to 8×10^{14} W/cm^2. The target H_2^+ molecule is in four different electronic states, and the internuclear distance is 2.0 a.u. The molecular axis $\boldsymbol{R}$ is fixed along the x component of the laser polarization vector (ε_x), so that $\theta_R = \pi/2$ and $\varphi_R = 0$ (Fig. 1(b)). The binding energies of the four electronic states are $E_b^{1s\sigma_g} = -1.1026$ a.u., $E_b^{1s\sigma_u} = -0.6675$ a.u., $E_b^{2p\pi_u} = -0.4288$ a.u., and $E_b^{2p\pi_g} = -0.2267$ a.u., respectively. According to Eq. (1), we calculate the 3D PADs by varying the polar angle θ_f from 0 to π, and the azimuthal angle φ_f from 0 to 2π in the polar coordinate.

Prior to showing the numerical results, we first study the electron distributions obtained by the LCAO for two purposes. One is to verify the validity of the LCAO treatment, and the other is for further comparison. Figure 2(a) shows the valence electron distribution of H_2^+ in a bonding electronic state $1s\sigma_g$. From Fig. 2(a), we can find that the valence electrons mainly accumulate along the molecular axis. Figure 2(b) depicts the 3D PAD of H_2^+ in $1s\sigma_g$ state for the photoelectron with a kinetic energy of 31.0 eV at the laser intensity of 8×10^{14} W/cm^2. The 3D PAD exhibits two identical balls located in the ε_y direction, which are regarded as the main lobes in this paper. There is no distribution of photoelectrons in the ε_x direction. From Fig. 2(a), we know that most of the valence electrons are located along the molecular axis, namely, along the ε_x axis, while few electrons are located along the ε_y axis. Surprisingly, we find that the electrons are not mainly ionized along the molecular axis. The destructive interference effect stemming from the molecular double-core structure brings about this phenomenon. Since the photoelectrons may come from any one of H_2^+ ions, two ionization channels form, and then the interference occurs between the two ionization channels. The interference behaves as a cosine function of $\boldsymbol{P}_f\cdot\boldsymbol{R}$, as shown in Eq. (5), which has a maximum along the direction vertical to the molecular axis ($\boldsymbol{R}$), because $\boldsymbol{P}_f\cdot\boldsymbol{R} = 0$. Therefore, in the direction vertical to the molecular axis $\boldsymbol{R}$, the interference effect is always constructive. On the contrary, along the molecular axis, the interference plays a destructive role because of $\cos(\boldsymbol{P}_f\cdot\boldsymbol{R}/2) = \cos(|\boldsymbol{P}_f\cdot\boldsymbol{R}/2|) \ll 1$ for the middle-energy photoelectrons, and thus suppresses the photoelectron yield. As a result, the photoelectron momentum spectra exhibit a $\pi/2$ rotation with respect to the molecular axis.

As discussed above, we have known that if $\cos(\boldsymbol{P}_f\cdot\boldsymbol{R}/2) = \cos(|\boldsymbol{P}_f\cdot\boldsymbol{R}/2|) \ll 1$ along the molecular axis, the interference effect is destructive. Hence, few electrons can be ionized along the molecular axis. However, if $\cos(\boldsymbol{P}_f\cdot\boldsymbol{R}/2) = \cos(|\boldsymbol{P}_f\cdot\boldsymbol{R}/2|) < 1$, some photoelectrons can be found along the molecular axis. In order to test this, we have calculated the 3D PAD for photoelectrons with an energy of 60.0 eV at laser intensity of 8×10^{14} W/cm^2, as shown in Fig. 3(a). Figure 3(a) demonstrates this striking feature that some of the photoelectrons emit out along the molecular axis, which forms a pair of jets sticking out from the waist of the main lobes. For a photoelectron with an energy of 60.0 eV, the value of $|P_f||R|$ exceeds π, and then $\cos(\boldsymbol{P}_f\cdot\boldsymbol{R}/2) = \cos(|\boldsymbol{P}_f\cdot\boldsymbol{R}/2|) < 1$, so a pair of jets along the molecular axis can be seen. We also think that as the kinetic energy of photoelectrons increases, the jets will become more and more prominent, and finally reach the same size as the main lobes. Thus, in Fig. 3(b), we show the 3D PAD for photoelectrons with an energy of 75.0 eV at the same laser intensity as that used in Fig. 3(a). Figure 3(b) shows that the size of jet is almost equal to that of the main lobes. The observation of these jets becomes easier and possible now, owing to the development in detection technology and intense laser technology, which will be a strong support to the interference scenario.

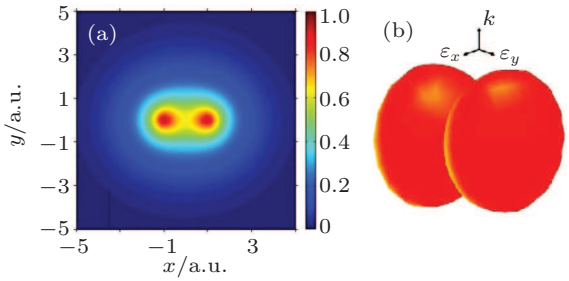


Fig. 2. (color online) (a) Contour plot of the valence electron distribution for H_2^+ molecule in $1s\sigma_g$ state in the xy plane. (b) The 3D PADs for photoelectrons with an energy of 31.0 eV at the laser intensity of 8×10^{14} W/cm^2. The two nuclei are located along the ε_x axis of the laser polarization vector. The laser field's wavelength is 0.8 μm. The inset in panel (b) shows the coordinate system of the laser field.

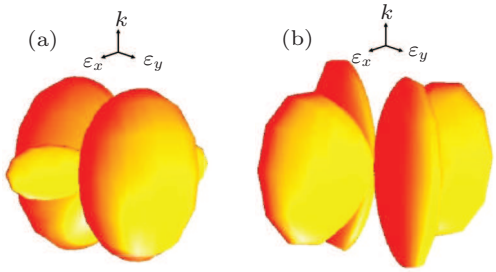


Fig. 3. (color online) The 3D PADs for photoelectrons with energies of (a) 60.0 eV and (b) 75.0 eV from H_2^+ molecule in $1s\sigma_g$ state. The molecular axis is along the ε_x axis. The laser field's wavelength is 0.8 μm, and its intensity is 8×10^{14} W/cm^2.

The above discussion is dedicated to the bonding electronic state. Now we divert our attention to molecules in antibonding electronic states by taking H_2^+ molecules in $1s\sigma_u$ electronic state as the initial state. The valence electrons of H_2^+ molecule in $1s\sigma_u$ electronic state are mostly located along the molecular axis, and the direction perpendicular to the molecular axis lies in the nodal plane, as shown in Fig. 4(a). Figure 4(b) shows the 3D PAD for photoelectrons with an energy

of about 31.0 eV at the laser intensity of 5×10^{14} W/cm^2. From the 3D PAD, we find that no main lobes appear in the ε_y direction, which means that there are no electrons emitting in this direction. However, there is a pair of jets along the ε_x direction, namely, along the molecular axis. That is to say, the PAD does not show any rotation with respect to the molecular axis to image the molecular orbital, which is the major difference between the $1s\sigma_g$ and the $1s\sigma_u$ electronic states. This phenomenon can be explained well by the interference scenario. The interference term of H_2^+ in $1s\sigma_u$ electronic state is a sine function in the form of $\sin(\boldsymbol{P}_f\cdot\mathbf{R}/2)$. In the direction vertical to the molecular axis, the interference term $\sin(\boldsymbol{P}_f\cdot\mathbf{R}/2)=0$ due to $\boldsymbol{P}_f\cdot\mathbf{R}/2=0$. Thus, the ionization yield is fully suppressed. On the contrary, in the direction along the molecular axis, the interference term takes the form of $\sin(|\boldsymbol{P}_f||\boldsymbol{R}|/2)$, and its value varies with the kinetic energy of photoelectrons. For photoelectrons with an energy of 31.0 eV, the value of $|\boldsymbol{P}_f||\boldsymbol{R}|$ is about π, and thus the interference maximum appears in the direction along the molecular axis. As the photoelectron energy increases, the value of $\sin(|\boldsymbol{P}_f||\boldsymbol{R}|/2)$ decreases, which causes the splitting of the jets of PAD along the molecular axis, as shown in Fig. 5. Figure 5 presents a 3D PAD at a photoelectron energy of about 69.75 eV. From this 3D PAD, we find that the jets along the molecular axis are split, which means that the ionization yield is suppressed in the molecular axis direction due to the destructive interference effect. If the photoelectron energy increases, the ionization yield will be completely suppressed along the molecular axis, and then the jets will be completely split. Here, we do not show this.

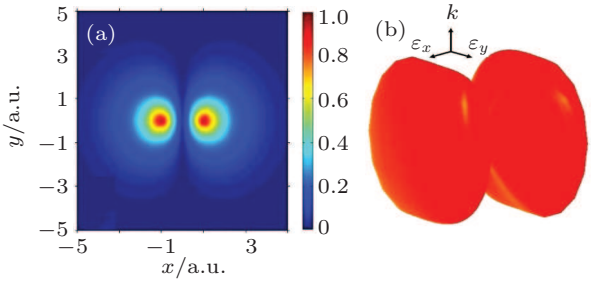


Fig. 4. (color online) (a) Contour plot of the valence electron distribution for H_2^+ molecule in $1s\sigma_u$ state in xy plane. (b) The 3D PAD for photoelectrons with the energy of 31.0 eV from H_2^+ molecule in $1s\sigma_u$ state. The laser field's wavelength is 0.8 μm, and its intensity is 5×10^{14} W/cm^2. The molecular axis is along the x component of laser polarization vector ε_x.

From the discussion above, we see that the corresponding relation between the PAD and the molecular axis drastically varies with the symmetric property of the molecular orbitals by calculating the PADs of H_2^+ molecules in both $1s\sigma_g$ and $1s\sigma_u$ electronic states, of which the valence electrons are concentrated along the internuclear axis, and around the two H cations. For comparative study of the other molecular orbitals, we study the photoionization of H_2^+ molecules in $2p\pi_u$ and $2p\pi_g$ electronic states, respectively. Their valence electrons are concentrated off the two H nuclei, as shown in Figs. 6(a) and 7(a).

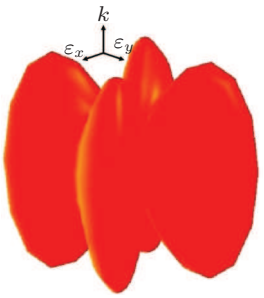


Fig. 5. (color online) The 3D PAD for photoelectrons with an energy of 69.75 eV from H_2^+ molecule in $1s\sigma_u$ state. The laser field's wavelength is 0.8 μm, and its intensity is 5×10^{14} W/cm^2. The molecular axis is along the x component of laser polarization vector ε_x.

The $2p\pi_u$ electronic state of H_2^+ molecule is a bonding electronic state. Its valence electrons are localized at the two sides of the molecular axis, and the molecular axis lies in the nodal plane, as displayed in Fig. 6(a). Figure 6(b) shows the 3D PAD for photoelectrons with an energy of 6.2 eV, which exhibits a pair of jets located in the ε_x axis. The photoelectrons are mainly ejected along this direction. The PAD imprints the molecular orbital after rotating a $\pi/2$ angle, which is similar to the case of H_2^+ in σ_g electronic state.

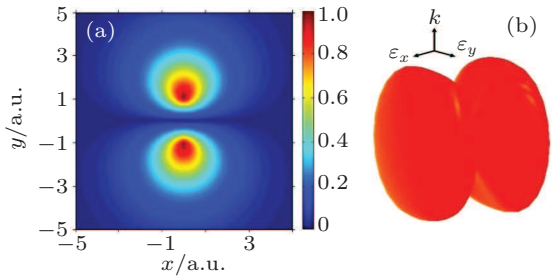


Fig. 6. (color online) (a) Contour plot of the valence electron distribution of H_2^+ molecule in $2\pi_u$ state in xy plane. (b) The 3D PAD for photoelectrons with an energy of 6.2 eV from H_2^+ molecule in $2p\pi_u$ state. The two nuclei are located along the ε_x axis. The laser field's wavelength is 0.8 μm, and its intensity is 4×10^{14} W/cm^2.

Figure 7(a) displays the valence electron distribution of H_2^+ molecules in $2p\pi_g$ electronic state. Two nodal planes appear in this distribution: one is parallel to the molecular axis, and the other is perpendicular to the molecular axis. The valence electrons are nearly located along the two diagonals of the xy plane, looking like a butterfly. Figure 7(b) shows the 3D PAD for photoelectrons with an energy of 6.2 eV, which is composed of four parts along the two diagonals. The ionization probability reaches a maximum in each quadrant, but is suppressed in the two nodal planes. In this case, the correspondence between the PADs and the distributions of valence electrons is clear, but the rotation of the PADs relative to the molecular axis is hard to identify.

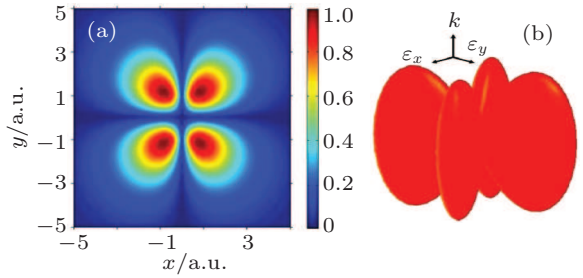


Fig. 7. (color online) (a) Contour plot of valence electron distribution of H_2^+ molecule in $2\pi_g$ state in xy plane. (b) The 3D PAD for photoelectrons with an energy of 6.2 eV from H_2^+ molecule in $2p\pi_g$ state. The two nuclei are located along the ε_x axis. The laser field's wavelength is 0.8 μm, and its intensity is 2×10^{14} W/cm^2.

4. Conclusions

In this paper, we theoretically study the strong-field ionization of the H_2^+ molecule in terms of the PAD, as well as its dependence on the kinetic energy of the photoelectron and the molecular orbital in four different electronic states in circularly polarized laser fields. The location of the main lobes of the PAD changes with the molecular orbitals. For molecules with bonding electronic states, the PAD generally shows a rotation of $\pi/2$ with respect to the molecular axis, while for molecules with antibonding electronic states, generally, no rotation occurs. We thus conclude that for molecules with bonding electronic states, the PAD imprints the molecular orbital after rotating a $\pi/2$ angle; while for molecules with antibonding electronic states, the PAD directly imprints the molecular orbital without any angle rotation. We use an interference scenario to interpret these phenomena. We also find that, due to the interference effect, a new pair of jets appears in the waist of the main lobes, and the main lobes or jets of PADs are split into two parts if the photoelectron energy is sufficiently high.

References

[1] Fittinghoff D N, Bolton P R, Chang B and Kulander K C 1992 *Phys. Rev. Lett.* **69** 2642

[2] Corkum P B 1993 *Phys. Rev. Lett.* **71** 1994

[3] Walker B, Sheehy B, DiMauro L F, Agostini P, Schafer K J and Kulander K C 1994 *Phys. Rev. Lett.* **73** 1227

[4] Pavićić D, Lee K F, Rayner D M, Corkum P B and Villeneuve D M 2007 *Phys. Rev. Lett.* **98** 243001

[5] Agostini P, Fabre F, Mainfray G, Petite G and Rahman N K 1979 *Phys. Rev. Lett.* **42** 1127

[6] Pei L and Guo C 2010 *Phys. Rev. A* **82** 021401

[7] Zhou Y M, Liao Q, Zhang Q B, Hong W Y and Lu P X 2010 *Opt. Express* **18** 632

[8] Ren X H, Zhang J T, Liu P, Wang Y and Xu Z Z 2009 *Phys. Lett. A* **373** 227

[9] Ren X H, Zhang J T, Wang Y, Xu Z Z and Guo D S 2009 *Eur. Phys. J. D* **51** 401

[10] Ren X H, Zhang J T, Wang Y, Xu Z Z, Wang J T and Guo D S 2010 *Chin. Phys. B* **19** 023202

[11] Zhang J T, Zhang W Q, Xu Z Z, Li X F, Fu P M, Guo D S and Freeman R R 2002 *J. Phys. B* **35** 4809

[12] Zhu X S, Zhang Q B, Hong W Y, Lu P X and Xu Z Z 2011 *Opt. Express* **19** 13722

[13] Holmegaard L, Hansen J L, Kalhøj L, Kragh S L, Stapelfeldt H, Filsinger F, Küpper J, Meijer G, Dimitrovski D, Abu-samha M, Martiny C P J and Madsen L B 2010 *Nature Phys.* **6** 428

[14] Martiny C P J, Abu-samha M and Madsen L B 2010 *Phys. Rev. A* **81** 063418

[15] Hansen J L, Holmegaard L, Kalhøj L, Kragh S L, Stapelfeldt H, Filsinger F, Meijer G and Küpper J 2011 *Phys. Rev. A* **83** 023406

[16] Shaaran T, Augstein B B and Figueira de Morisson Faria C 2011 *Phys. Rev. A* **84** 013429

[17] Dimitrovski D, Abu-samha M, Bojer Madsen L, Filsinger F, Meijer G and Jochen K 2011 *Phys. Rev. A* **83** 023405

[18] Slater J 1930 *Phys. Rev.* **36** 57

[19] Fernández J and Madsen L B 2009 *J. Phys. B* **42** 085602

[20] Picón A, Bahabad A, Kapteyn H C, Murnane M M and Becker A 2011 *Phys. Rev. A* **83** 013414

[21] Fojón O A, Fernandez J, Palacios A, Rivarola R D and Martin F 2004 *J. Phys. B* **37** 3035

[22] Yudin G L, Chelkowski S and Bandrauk A D 2006 *J. Phys. B* **39** L17

[23] Picca R D, Fainstein P D and Dubois A 2011 *Phys. Rev. A* **84** 033405

[24] Ren X H, Zhang J T, Liu P, Wang Y and Xu Z Z 2008 *Phys. Rev. A* **78** 043411

[25] Milošević D B 2006 *Phys. Rev. A* **74** 063404

[26] Reiss H R 1980 *Phys. Rev. A* **22** 1786

[27] Becker A and Faisal F H M 2005 *J. Phys. B* **38** R1

[28] Wolkov D M Z 1935 *Z. Phys.* **94** 250

[29] Jaroń-Becker A, Becker A and Faisal F H M 2004 *Phys. Rev. A* **69** 023410

[30] Usachenko V I 2006 *Phys. Rev. A* **73** 047402

[31] Kamta G L and Bandrauk A D 2006 *Phys. Rev. A* **74** 033415

[32] Muth-Böhm J, Becker A and Faisal F H M 2000 *Phys. Rev. Lett.* **85** 2280